Optimization of concentrations of natural antioxidants (curcumin) to enhance the thermal stability of ultra high molecular weight polyethylene (UHMWPE)

Nidhi Khattar[1] · Jagriti[1] · Shagun Kainth[2] · Piyush Sharma[3] · Vishal Ahlawat[4] · Urmila Berar[1] · Pawan K. Diwan[1]

Abstract

The impact of different concentrations of natural antioxidants (curcumin) on the thermal stability of UHMWPE (ultra-high molecular weight polyethylene) is examined via the thermogravimetric (TGA/DTA) technique, in the temperature region 50–600 °C at a 5 °C/min heating rate. This work employs the model fitting (Coats and Redfern) approach to determine the optimal curcumin concentration. UHMWPE samples at optimum concentration are further subjected to three other heating rates, viz., 10, 15 and 20 °C. A bi-Gaussian asymmetric function is utilized for deconvolution to elucidate the complexities of thermal decomposition. Through deconvolution, two peaks are obtained and the activation energy corresponding to each peak is determined through two iso-conversional kinetic (Friedman and Starink) models. By utilizing activation energy, the random nucleation reaction mechanism involved in thermal decomposition is recognized. Finally, changes in entropy (ΔS), enthalpy (ΔH) and Gibbs free energy (ΔG) are determined.

Keywords Curcumin · UHMWPE · Deconvolution · Kinetic triplets · Thermodynamic parameters

✉ Pawan K. Diwan
diwanpk74@gmail.com

1   Department of Applied Science, UIET, Kurukshetra University, Kurukshetra 136 119, India

2   School of Chemical Engineering and Physical Sciences, Lovely Professional University, Phagwara 144 411, India

3   School of Mechanical Engineering, Lovely Professional University, Phagwara 144 411, India

4   Department of Mechanical Engineering, UIET, Kurukshetra University, Kurukshetra 136 119, India

🙋 Springer

Introduction

Natural antioxidants, usually found in vegetables, fruits, herbs, spices, tea leaves, etc., have great potential to minimize the oxidative damage to polymeric materials, mainly polyolefins, by scavenging free radicals in several ways, including hydrogen atom transfer (HAT), radical adduct formation (RAF), and single electron transfer (SET) [1–3]. The majority of natural antioxidants are reported to have phenol derivatives with more than one hydroxyl group, attached to an aromatic ring [4, 5]. These phenolic compounds donate hydrogen to the free radicals formed during the thermo-oxidative degradation of polyolefins. This results in the formation of resonance-stabilized phenoxy radicals, which subsequently react with other free radicals to form adducts. A phenolic compound's antioxidant activity can be altered by changing the position of -OH groups and the nature of substituents on the aromatic scaffold. For instance, in contrast to meta positions, -OH groups attached to ortho and para positions offer more hydrogen atoms to free radicals. Further, by adding electron donating groups to the phenolic ring, the availability of electrons is increased, which improves the antioxidant activity of the compound [6]. On the other hand, electron withdrawing groups can stabilize the phenolic radical that is formed during the antioxidant process, which can reduce antioxidant activities [7]. Therefore, due to diverse structural arrangements, phenolic compounds can be categorized into different categories, viz. Phenolic acid, Acetophenones, Phenylacetic acids, Hydroxycinnamic acids, Coumarins, Naphthoquinones, Xanthones, Stilbenes, Flavonoids, etc. Researchers tried all these phenolic compounds as antioxidants to enhance the thermo-oxidative stability of polymeric materials and found that flavonoids are more effective as compared to other antioxidants [8, 9].

Generally, the structures of flavonoids consist of 15 carbons, with two benzene rings connected to one pyran ring. However, there are also other types of flavonoids that are open chains, like chalcone, which possesses two aromatic (benzene) rings connected through an unsaturated carbonyl group. One of the chalcones known as curcumin [1E,6E)-1,7-bis(4-hydroxy-3-methoxyphenyl)-1,6-heptadiene-3,5-dione] extract from turmeric, has gained attention as an antioxidant due to the arrangement of the -OH group and subsequent changes in its structure. In curcumin, the phenolic group is sterically hindered due to the presence of two methoxy groups at ortho position of the benzene ring [10–12]. Due to the unique structure of curcumin, it is widely utilized as a polyethylene stabilizer. Research on curcumin has explored its thermal stability, spectroscopic properties, and degradation kinetics under various conditions. Thermogravimetric analysis revealed curcumin's mass loss occurs between 509 and 673 K [13]. The concentration and temperature of curcumin affect its spectroscopic properties in liposomal form, with higher temperatures leading to decreased absorption intensity but increased fluorescence anisotropy [14]. Curcumin's antioxidant efficiency in soybean oil improves with increasing concentration, showing comparable activity to α-tocopherol and TBHQ at 25 °C in darkness [15]. The degradation of curcumin follows first-order kinetics, with rate increasing at higher pH, temperature,

and dielectric constant. Notably, curcumin loaded in polymeric micelles exhibited 300–500 times greater stability compared to aqueous buffer, suggesting a promising approach for pharmaceutical applications [16]. These findings contribute to understanding curcumin's behavior under various conditions and its potential for stabilization. However, no study related to the effect of curcumin concentration on the rate of mass loss at different temperatures has been examined.

In the present study, curcumin at different wt% is blended in an UHMWPE (ultra-high molecular weight polyethylene) matrix and subjected to TGA/DTA analysis at a 5 °C/min heating rate for estimation of the rate of mass loss and determination of activation energy using the Coats and Redfern kinetic model. Through this, optimal curcumin's concentration is identified for protecting UHMWPE from oxidative degradation and for better usage in different industries and engineering applications [17–20]. UHMWPE with an optimal concentration of curcumin is further studied at other heating rates (10, 15, 20 °C/min) adopting the deconvolution technique to resolve the complexities involved in the reaction mechanism, during thermal decompositions. Following deconvolution, Friedman and Starink kinetic models determine the activation energies corresponding to each peak. Finally, the reaction mechanism is identified and thermodynamic parameters like change in entropy (ΔS), change in enthalpy (ΔH) and change in Gibbs free energy (ΔG) are determined.

Material and methodology

Material

UHMWPE (ultra-high molecular weight polyethylene) and curcumin powder are procured from Sigma Aldrich Co. USA. The molecular weight of UHMWPE powder is 3,000,000–6,000,000 g/mol and its density is 0.94 g/ml. The quoted percentage purity of curcumin is $\geq 98\%$.

Sample preparation

Curcumin weighing 0.05 to 0.5 g is added to ethanol at intervals of 0.05 g to get a 1 wt% dark yellow colour solution. In this way, ten UHMWPE-Curcumin (C) samples with varying concentrations (0.1 to 1.0 wt%) are obtained by mixing curcumin-ethanolic solution with UHMWPE powder. The ethanolic-curcumin solution is adequately homogenized in the UHMWPE matrix by utilizing a magnetic stirrer for 30 min. Afterwards, the mixture is dried in an oven at 50 °C to evaporate the ethanol. The dry UHMWPE-C powder is kept overnight in desiccators with anhydrous blue silica gel for viable ethanol elimination [21].

Moulding of the sample

Dried UHMWPE—C powder is first compacted in a cylindrically designed (diameter: 12 mm; height: 40 mm) mould at a 5 MPa pressure and 25 °C temperature and then

compressed at an optimized pressure–temperature (pressure: 15 MPa, temperature: 140 °C) combination [22]. These samples are gradually cooled over a dwell time of 10 min. and finally cut with a sharp blade to obtain ~ 0.5 mm thickness for each sample.

Thermogravimetric analysis (TGA)

Thin (~ 0.5 mm thickness) samples were placed in an alumina crucible, one by one, and subjected to thermogravimetric analysis (TGA) in a nitrogen environment with a 100 ml/min. flow rate. The mass loss of these samples is recorded as a function of temperature at a 5 °C/min. heating rate in the temperature range of 50–600 °C. In addition, samples having maximum thermal stability are further subjected to thermogravimetric analysis at three different heating rates, viz., 10, 15 and 20 °C /min. Finally, these recorded thermograms are analyzed by utilizing the ORIGIN software.

Theoretical approach

Identification of most thermally stable sample

To determine activation energy at different curcumin concentrations, the Coats and Redfern (CR) [23] kinetic model is employed. This model is used to identify most thermally stable sample. The sample with highest activation energy value exhibit highest thermal stability. The model relates reaction rate (α) with sample temperature (T) through the following equation:

$$ln\left(\frac{-ln(1-\alpha)}{T^2}\right) = ln\left(\frac{AR}{\beta E_a}\right) + ln\left(1 - \frac{2RT}{E_a}\right) - \frac{E_a}{RT} \qquad (1)$$

A, R, β and E_a represent Arrhenius pre-exponential factor (min^{-1}), gas constant (8.314 J mol^{-1} K^{-1}), linear heating rate (°C /min) and activation energy (kJ mol^{-1}).

Thermal kinetic parameters of UHMWPE at an optimized curcumin concentration

A detailed kinetic analysis is performed after identifying the most thermally stable sample by using the deconvolution technique. This process enables separation overlapping thermal events in a complex thermogravimetric analysis (TGA) curve. Afterwards, thermal kinetic parameters (activation energy, pre-exponential factor and reaction mechanism) are determined for the most thermally stable sample at multiple heating rates. The details of deconvolution technique and calculation of thermal kinetic parameters are as follows:

Deconvolution technique

It also helps in identifying the complexity involved in thermal decomposition, which is resolved through the deconvolution technique adopting an asymmetric bi-Gaussian distribution function, which is expressed as

$$y = \begin{pmatrix} y_0 + He^{-0.5\left(\frac{x-x_c}{w_1}\right)^2} \ for \ x < x_c \\ y_0 + He^{-0.5\left(\frac{x-x_c}{w_2}\right)^2} \ for \ x \geq x_c \end{pmatrix} \tag{2}$$

y_0 represent baseline, H maximum height, x independent variables, x_c central value, w_1 and w_2 are left and right-side widths in Gaussian distribution.

Activation energy

After deconvolution, the activation energies of distinguished peaks are determined through the differential (Friedman) model [24]

$$ln\left(\beta\frac{d\alpha}{dT}\right) = lnA + lnf(\alpha) - \frac{E_a}{RT} \tag{3}$$

and integral (Starink) model [25]

$$ln\left(\frac{\beta}{T^{1.92}}\right) = ln\left(\frac{AR}{E_a}\right) + ln\left(\frac{df(\alpha)}{d\alpha}\right) - 1.0008\frac{E_a}{RT} \tag{4}$$

Estimation of the reaction mechanism

By utilizing activation energy, the reaction mechanism is estimated through integral and master plots as:

$$g(\alpha) = \frac{AE_a}{\beta R}P(u) \tag{5}$$

$g(\alpha)$ is the integral function of degree of conversion, $u = \frac{E_a}{RT}$ and $P(u)$ is expressed as

$$P(u) \approx \frac{\exp(-1.0008u - 0.312)}{u^{0.92}} \tag{6}$$

Finally, the following expression identifies the reaction mechanism:

$$\frac{g(\alpha)}{g(0.5)} = \frac{P(u)}{P(0.5)} \tag{7}$$

Through comparison between experimental $\left(\frac{P(u)}{P(0.5)}\right)$ and theoretical master $\left(\frac{g(\alpha)}{g(0.5)}\right)$ curves, the exact reaction mechanism occurs during the thermal decomposition of UHMWPE-C sample is identified.

Pre-exponential factor and thermodynamic parameters

The identified reaction mechanism ($g(\alpha)$) is utilized to determine the pre-exponential factor (A) through Eq. 5.

For thermodynamic parameters such as change in entropy (ΔS), change in enthalpy (ΔH) and change in Gibb's free energy (ΔG), following mathematical equations [26, 27] are utilized.

$$\Delta S = Rln\left(\frac{Ah}{e\chi k_B T_{max}}\right) \tag{8}$$

$$\Delta H = E_a - RT_{max} \tag{9}$$

$$\Delta G = \Delta H - T_{max}\Delta S \tag{10}$$

h is Planck constant, k_B is Boltzmann's constant, e is Neper number, χ is transition number and T_{max} is maximum decomposition temperature.

Results and discussion

Curcumin as an antioxidant/pro-oxidant

At different concentrations, curcumin in the UHMWPE matrix behaves differently. At low concentrations, curcumin quenches reactive oxygen species (ROS) production and acts as antioxidant whereas at higher concentrations, it induces ROS production and behaves as a pro-oxidant [5]. As observed in Fig. 1, curcumin shows its effective antioxidant activity by shifting the mass loss curves of UHMWPE towards the higher temperature side up to 0.2 wt%. Following further increases in curcumin concentration (0.3–0.5 wt%), mass loss curves shifted to the lower temperature side.
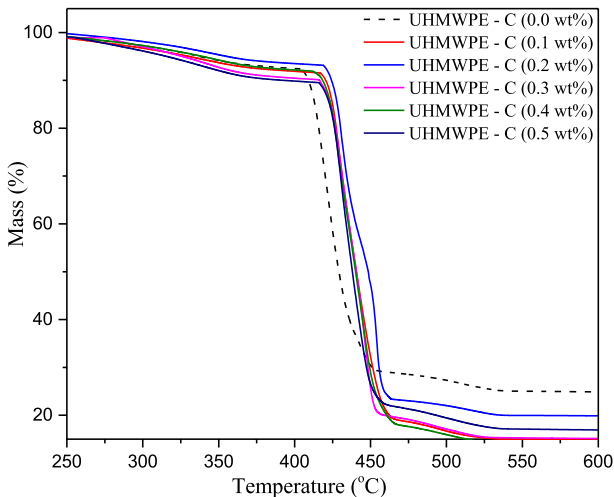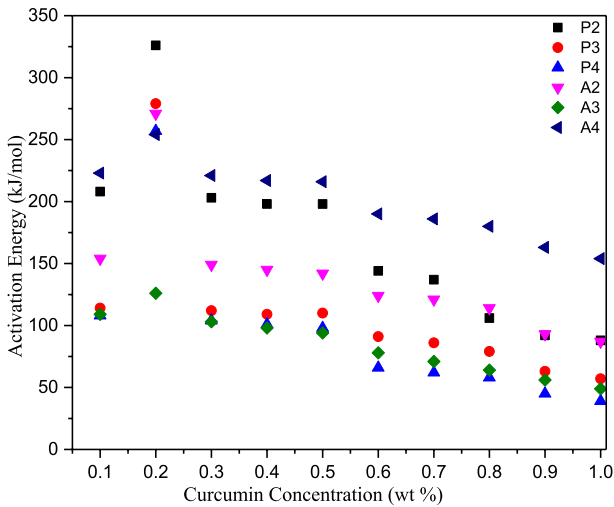

Fig. 1 Mass-loss/Thermogravimetric (TG) curves of UHMWPE blended with 0.0–0.5 wt% curcumin concentration

Table 1 Nucleation reaction mechanisms and corresponding integral functions $g(\alpha)$

Reaction Mechanism	$g()$
Power law (P2)	$1/2$
Power law (P3)	$1/3$
Power law (P4)	$1/4$
Avrami-Erofeev (A2)	$[-ln(1-)]^{1/2}$
Avrami-Erofeev (A3)	$[-ln(1-)]^{1/3}$
Avrami-Erofeev (A4)	$[-ln(1-)]^{1/4}$

Fig. 2 Activation energy values, as a function of curcumin concentration, based on Coats and Redfern kinetic model adopting different nucleation reaction mechanisms

Moreover, as shown in Fig.S1, 0.6–1.0 wt% of curcumin shifted the mass loss curves even below the mass loss curve of pure UHMWPE.

The shift in mass loss curves towards the higher temperature side at low concentrations is due to the presence of electron releasing methoxy groups and their π-conjugation in the aromatic ring of curcumin. These are responsible for releasing H^+ ions and quenching the reactive oxygen species (ROS). Whereas, at higher concentrations, α, β unsaturated carbonyl moiety of curcumin produces a variety of ROS and accelerates the pro-oxidant activity [28, 29]. Above discussion reveals that antioxidant-activity or thermal-stability is at its maximum at 0.2 wt% curcumin concentration. At this concentration, the maximum decomposition is 437 °C.

In order to ascertain that the thermal stability of UHMWPE is maximum at 0.2 wt% curcumin concentration only, the mass loss curves at different concentrations are further explored to determine activation energy by utilizing the Coats and Redfern kinetic model adopting different nucleation reaction mechanisms (Table 1). Fig. 2 reveals higher activation energy values at 0.2 wt% for the considered reaction

mechanisms. Higher activation energy values reveal that curcumin at 0.2 wt% has the best antioxidant activity to thermally stabilize the UHMWPE.

Thermal kinetic parameters of UHMWPE at 0.2 wt% curcumin concentration

Mass-loss/thermogravimetric (TG) and its derivative (DTG) curve, of UHMWPE blended with 0.2 wt% curcumin, are presented in Fig. 3. It reveals that the thermal decomposition process occurs in three stages. In Stage-I (~ 50–240 °C), no mass loss is observed. The second stage (Stage-II) lies between temperatures 240 to 539 °C. This stage is very active and entails complex decomposition processes. As the temperature increases, free radicals are quenched and accordingly, different stable products of low molecular weight are formed. Further, the sample completely volatized in stage-III and no mass loss occurred.

For better understanding of kinetic parameters, thermograms of UHMWPE–Curcumin (0.2 wt%) at four different heating rates (5, 10, 15, 20 °C/min.) are obtained (Fig. S2). From this fig., it is observed that thermal decomposition curves shifted towards the higher temperature side with an increase of heating rate. This is due to the delayed participation of radicals in thermal decomposition processes. The complexities involved in Stage-II are resolved through the deconvolution technique adopting a bi-Gaussian asymmetric function (Eq. 2). Through this, two peaks are observed at a 5 °C/min heating rate; one at 422 °C and the other at 445 °C (Fig. 4). In the same way, two peaks are also observed for other heating rates (10, 15 and 20 °C/min) (Fig. S3). The value of R^2 was found to be
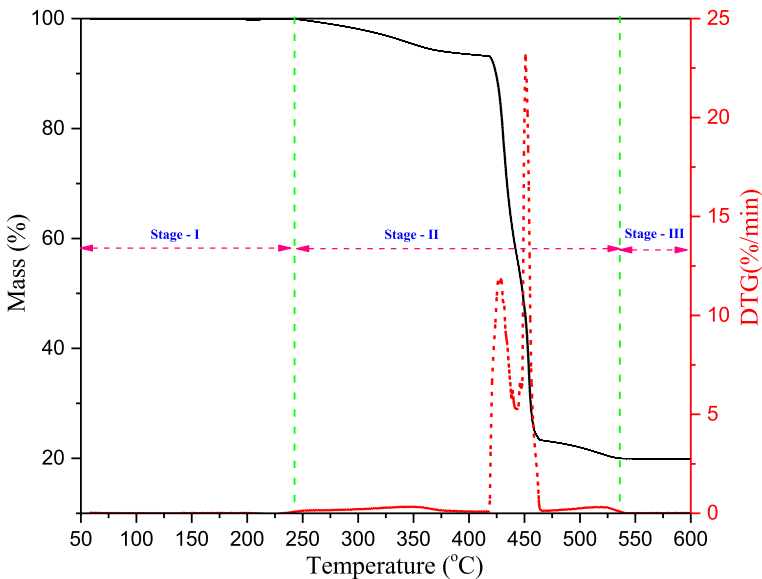

Fig. 3 Mass Loss/Thermogravimetric (TG) and Derivative Thermogravimetric (DTG) curves of UHMWPE blended with 0.2 wt% curcumin, at 5 °C/min heating rate
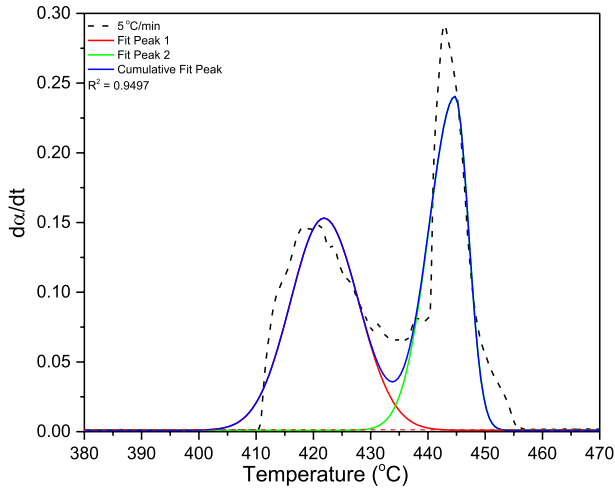
Fig. 4 Deconvolution of Stage-II of thermograms obtained at 5 °C/min. heating rate

greater than 0.9 in all the deconvoluted samples (Fig. 4 and S3). The first peak typically represents the initial degradation of lower molecular weight fractions or additives, while the second peak corresponds to the decomposition of the main polymer backbone. Further, the rate of degree of conversion ($d(\alpha)/dt$) as a function of sample temperature are presented in Fig. 5 & S4 for Peak 1 and Peak 2, respectively. It also observes that the peaks shift towards the higher temperature side, thereby supporting the thermal lagging hypothesis.
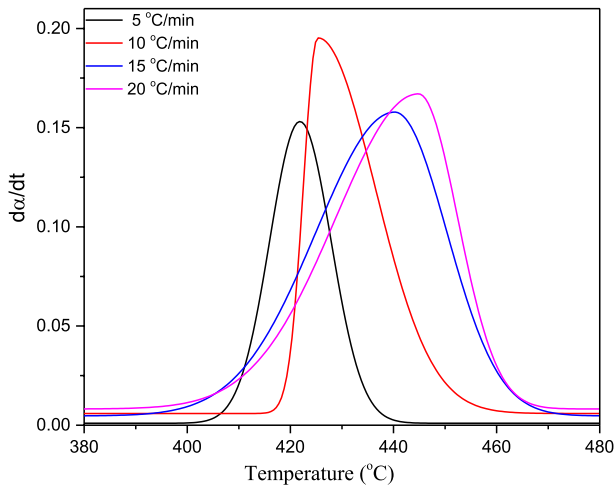

Fig. 5 Rate of degree of conversion ($d\alpha/dt$) as a function of sample temperature for Peak 1, at considered heating rates
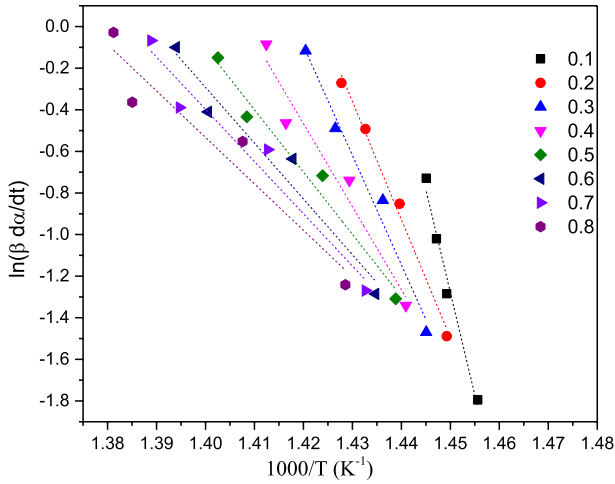
Fig. 6 Linear fitted plots at different degree of conversions (α) obtained through Friedman kinetic model for Peak 1
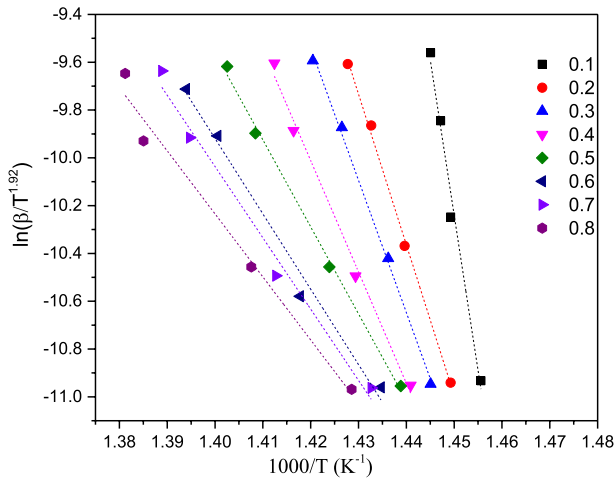

Fig. 7 Linear fitted plots at different degree of conversions (α) obtained through Starink kinetic model for Peak 1

Estimation of activation energy

By utilizing degree of conversion (α) values, obtained through Figs. 5 and S4, and adopting Friedman and Starink models, the linear fitted plots (Figs. 6, S5, 7 and S6) for Peak 1 and Peak 2 are generated. Through the slopes of these plots, activation energy values at different degrees of conversion (α) values are determined and presented in Figs. 7 and S7. Activation energy decreases with an increase in

the degree of conversion, irrespective of peaks and kinetic models. However, the activation energy of Peak 1 is higher than Peak 2.(Fig. 8)

Identification of the exact reaction mechanism

Using Starink-model based activation energy, experimental points are obtained and presented in Figs. 9 and S8 as a function of degree of conversion (α) at four different heating rates. In this figure, theoretical master curves (Eq. 7) generated through considered reaction mechanisms (Table 1) are also incorporated. Comparison reveals that Peak 1 and Peak 2 adhere to the A2 and A4 (random nucleation) reaction mechanisms, respectively. These reaction mechanisms may be due to the semi-crystalline nature of UHMWPE. These reaction mechanisms restrict the free radical mobility in the amorphous phase and as a result, a higher nucleation rate occurs, which leads to more nucleation sites as well as accelerates random nucleation processes [30].

Determination of pre-exponential factor and thermodynamic parameters

Through identified reaction mechanisms, pre-exponential factors are determined by replacing $g(\alpha)$ (Eq. 5) with A2 and A4 reaction mechanisms for Peak 1 and Peak 2 respectively via following equations:

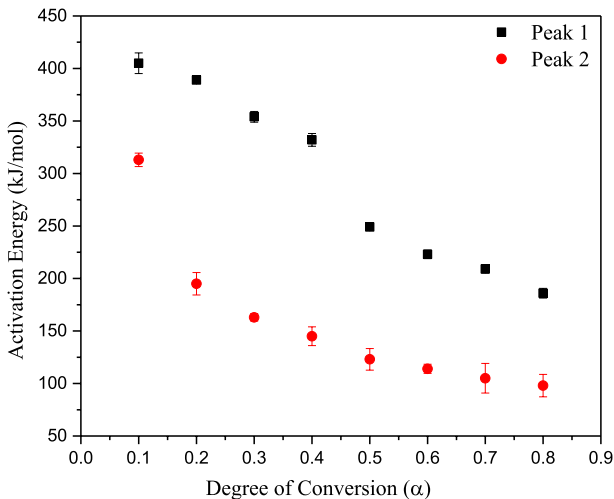$$[-ln(1 - (\alpha))]^{1/2} = \frac{AE_a}{\beta R}P(u) \tag{11}$$

Fig. 8 Variation of activation energy as a function of degree of conversion (α) of Peak 1 and Peak 2 for Friedman kinetic model
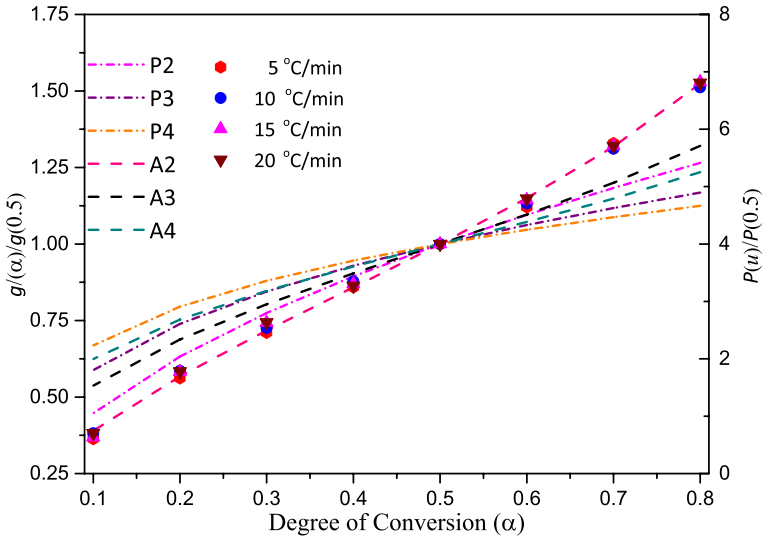
Fig. 9 Comparison between experimental points and theoretical master's curves obtained for different nucleation reaction mechanisms for Peak 1

$$[-ln(1-(\alpha))]^{1/4} = \frac{AE_a}{\beta R}P(u) \tag{12}$$

By plotting linear fitted curves between $[-ln(1-(\alpha))]^{1/2}$ and $(E_a/\beta R)P(u)$ for Peak 1 (Fig. 10) and $[-ln(1-(\alpha))]^{1/4}$ and $(E_a/\beta R)P(u)$ for Peak 2 (Fig. S9, pre-exponential factors at 5 °C/min heating rate are determined. Similarly,
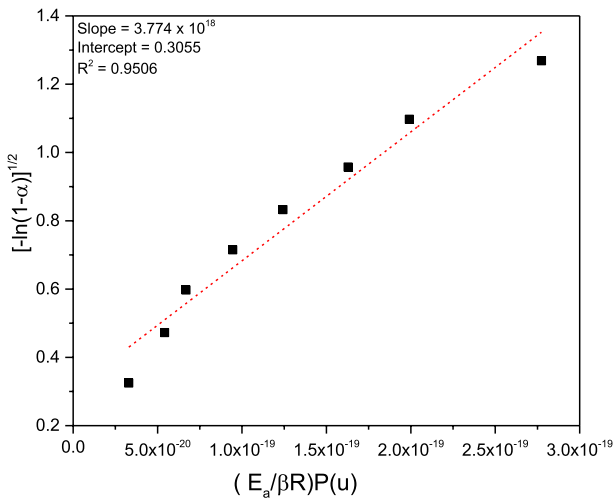

Fig. 10 Linear fitted curves to obtain pre-exponential factors at 5 °C/min heating rate for Peak 1

Table 2 Pre-exponential factor and thermodynamic parameters of Peak 1 at different heating rates

Heating Rate (°C/min)	T_{max} (°C)	A (1/min)	ΔS (J/mol/K)	ΔH (kJ/mol)	ΔG (kJ/mol)
5	422	3.77×10^{18}	95.37	221.70	155.42
10	426	4.32×10^{18}	96.45	221.37	153.96
15	440	6.24×10^{18}	99.34	220.21	149.38
20	445	8.45×10^{18}	101.80	219.79	146.70

Table 3 Pre-exponential factor and thermodynamic parameters of Peak 2 at different heating rates

Heating Rate (°C/min)	T_{max} (°C)	A (1/min)	ΔS (J/mol/K)	ΔH (kJ/mol)	ΔG (kJ/mol)
5	445	8.90×10^{13}	6.78	169.23	164.52
10	455	1.16×10^{14}	8.91	168.90	162.67
15	469	1.83×10^{14}	12.55	167.74	158.79
20	471	3.58×10^{14}	18.08	167.32	154.34

pre-exponential factors for other considered heating rates are determined and presented in Table 2 & Table 3 of Peak 1 and Peak 2, respectively. Thermodynamic parameters (enthalpy, entropy and Gibb's free energy) are determined through Eqs. 8, 9 and 10 and given in Tables 2 and 3, as a function of heating rate. In chemical reactions, the change in enthalpy is associated with the heat exchanged with the surroundings, making it a key factor in studying reaction energetics. The entropy quantifies the number of possible microscopic configurations that correspond to a thermodynamic system's macroscopic state. Moreover, Gibbs free energy change (ΔG) predicts the spontaneity of a process. The positive values of ΔS, ΔG and ΔH indicate that thermal decomposition, of UHMWPE blended with 0.2 wt% of curcumin, is non-spontaneous.

Conclusions

Curcumin's blending into UHMWPE matrix does not influence the thermal decomposition stages, though the temperature regions of these stages are different at different curcumin concentrations. Curcumin works as a pro-oxidant in UHMWPE at higher concentrations (0.6–1.0 wt%). The Coats-Redfern model revealed that the sample with 0.2 wt% curcumin concentration exhibit maximum thermal stability. The complexity involved in the main stage of decomposition (Stage-II) for the sample with 0.2 wt% curcumin concentration is resolved through deconvolution technique. The result revealed overlapping of two peaks in stage II of thermal decomposition. The first peak is associated with breakdown of lower molecular weight fractions or additives, while the second peak signifies the degradation of the main polymer structure. Additionally, both the integral (Starink model) and differential (Friedman) kinetic models determine a similar trend in activation energy with varying degrees of conversion values, validating the

activation energy calculation. Thermal decomposition of UHMWPE, blended with 0.2 wt% curcumin, followed random nucleation mechanisms. Further, observed thermodynamic parameters indicate that thermal decomposition is non-spontaneous, endergonic, and unfavorable. The study will be useful to enhance the thermal stability of UHMWPE as well as this approach can be applied to various materials, paving the way for further research and innovation in high-temperature applications.

Supplementary Information The online version contains supplementary material available at https://doi.org/10.1007/s11144-024-02697-9.

Data availability Data will be made available on request.

References

1. Kirschweng B, Tátraaljai D, Földes E, Pukánszky B (2017) Poly Degrad Stab 145:25–40
2. Molski M (2023) Heliyon 9:e12806
3. Brito J, Hlushko H, Abbott A, Aliakseyeu A, Hlushko R, Sukhishvili SA (2021) ACS Appl Mater Interf 13(35):41372–41395
4. Nagarajan S, Nagarajan R, Kumar J, Salemme A, Togna AR, Saso L, Bruno F (2020) Polymers 12(8):1646
5. Malik P, Mukherjee TK (2014) J Biol 2014:1–8
6. Kajiyama T, Ohkatsu Y (2021) Poly Degrad Stab 71(3):445–452
7. Lee CY, Anamoah C, Semenya J, Chapman KN, Knoll AN, Brinkman HF, Malone JI, Sharma A (2020) Tetrahedron Lett 61(11):151607
8. Sun W, Shahrajabian MH (2023) Molecules 28(4):1845
9. Masek A, Plota A (2021) Int J Mol Sci 22(8):4018
10. Fujisawa S, Atsumi T, Ishihara M, Kadoma Y (2004) Anticancer Res 24(2B):563–570
11. Kirschweng B, Tátraaljai D, Földes E, Pukánszky B (2015) Poly Degrad Stab 118:17–23
12. Alven S, Nqoro X, Aderibigbe BA (2020) Polymers 12(10):2286
13. El-Menyawy EM, Raslan M, Zedan IT, Desoky WM (2024) ECS. J Solid State Sci and Tech 13(1):013003
14. Niu Y, Wang X, Chai S, Chen Z, An X, Shen W (2012) J Agri Food Chem 60(7):1865–1870
15. Eshghi N, Asnaashari M, Haddad Khodaparast MH, Hosseini F (2014) Natur Prod Res 28(17):1375–1378
16. Naksuriya O, van Steenbergen MJ, Torano JS, Okonogi S, Hennink WE (2016) The AAPS J 18:777–787
17. Shammazov I, Karyakina E (2023) Fluids 8:68
18. Piska M, Urbancova K (2022) Mach 10:1008
19. Zhimin Y, Xincong Z, Hongling Q, Wanying N, Hao W, Kai L, Yumin T (2015) Wear 332:872–878
20. Chu Y, Chen X, Tian L (2017) Appl Surf Sci 406:77–83
21. Van Mourik JH (1965) Am Ind Hyg Assoc J 26:498–509
22. Khattar N, Jagriti, Ahlawat V, Sharma P, Berar U, Diwan PK (2023) Mater Chem Phys 10:128220 (1–9)
23. Coats AW, Redfern JP (1964) Nature 201:68–69
24. Friedman HL (1964) J Polym Sci Part C Polym Symp 6:183–195
25. Starink MJ (2003) Thermochim Acta 404:163–176
26. Georgieva V, Zvezdova D, Vlaev L (2013) J Therm Anal Calorim 111:763–771
27. Sharma P, Pandey OP, Diwan PK (2019) Fuel 253:1149–1161
28. Sandur SK, Ichikawa H, Pandey MK, Kunnumakkara AB, Sung B, Sethi G, Aggarwal BB (2007) Free Radic Boil Med 43(4):568–580
29. Kunwar A, Barik A, Sandur SK, Indira Priyadarsini K (2011) Free Radic Res 45(8):959–965
30. Xu J, Reiter G, Alamo RG (2021) Crystals 11:304